Elsevier Editorial System(tm) for Analytica Chimica Acta
Manuscript Draft

Manuscript Number: ACA-11-2023R2

Title: Immobilization of chitosan in sol-gel phases for chiral open-tubular capillary electrochromatography

Article Type: Full Length Article

Section/Category: SEPARATION METHODS

Keywords: Capillary electrochromatography; Chiral stationary phase; Chitosan; Open-tubular; Sol-gel

Corresponding Author: Dr. Jian-Lian Chen,

Corresponding Author's Institution: China Medical University

First Author: Jian-Lian Chen

Order of Authors: Jian-Lian Chen; Hong-Jie Syu

Suggested Reviewers: Joseph J. Pesek
Department of Chemistry, San Jose State University
pesek@sjsu.edu

Ute Pyell
Department of Chemistry, University of Marburg
pyell@chemie.uni-marburg.de

Norman William Smith
PhaPharmaceutical Science Division,, King's College
norman.2.smith@kcl.ac.uk

Hsin-Lung Wu
School of Pharmacy, Kaoshiung Medical University
hlwu@kmu.edu.tw

December 26, 2011

Editorial Office

Analytica Chimica Acta

Dear Editor,

We decide not to change the form of last revision, ACA-11-2023R1 and hope the reasons given in the file “Response to Reviews” could be accepted by you and referees.

Thank you for the kind re-consideration of suitability for publication of this manuscript in your esteemed journal.

Sincerely yours,

Jian-Lian Chen

Professor,

School of Pharmacy, China Medical University

***Response to Reviews**

Comment: The authors have addressed the concerns of reviewers 1 and 3 but not of reviewer 2. This reviewer questioned the apparently negative k" values, which indicate that each enantiomer's mobility is faster than the sum of its electrophoretic mobility and the electrosomotic mobility of the electrolyte.

The authors in their response cite several papers of their own, and 3 papers by different authors where a negative k' value is observed in LC and attributed to electrostatic repulsion between the analyte and the stationary phase. It should be noted that repulsion alone is not the mechanism repsonsible for the negative k' in packed-column LC, but rather it is due to Donnan exclusion: the exclusion of the analyte from the pore volume of the stationary phase, while the void marker does permeate through the pore volume.

It is by no means clear that Donnan exclusion should lead to decreased retention times for the enantiomers in the current CEC work, since there is not a packed column but an open tubular one (for column I, the authors explicity state that the 'bonded phase was only constructed of a molecular layer of chitosan'). Why then should the (unspecified) neutral marker permeate more slowly than the analyte enantiomers (ignoring the electrophoretic influence)? It does not travel a longer route, as might be the case in packed-column LC.

I concur with reviewer 1 that the neutral marker is in fact interacting with the stationary phase leading to an incorrect value of t0.

The authors clearly have no intention of doing any additional experiments to support their work. However, if the results are to be published in their current form, I believe they must offer a fuller explanation of the negative k" values along the lines of the above.

Response: Donnan exclusion mechanism is mostly found in ion-exclusion chromatography. When an ion-exclusion column is filled with aqueous buffers as a mobile phase, the water molecules accumulate as hydration spheres around the dissociated functional groups of the polymer support. By analogy with the Donnan membrane equilibrium, the hydrated polymer network behaves as a semi-permeable membrane between the stationary and mobile phases. Water, contained in the “pores” of the support and in the hydration spheres, is immobilized, thus forming the stationary phase. For convenience, the trapped liquid is referred to be in the

“pores”, but use of this term does not imply that a physical pore exists in the polymeric structure. Neutral, uncharged molecules penetrate through the “pore”, while similarly charged co-ions are repulsed by the presence of dissociated functional groups immobilized in the stationary phase. [J. Sep. Sci. 2003, 26, 1547–1553; J. Chromatogr. A, 2006, 1118, 19–28] All our studied phases (I, II, and III) were synthesized through sol-gel polymerization. The sol-gel based phases are more hydrophilic than the organic polymer based ones used in ion-exclusion chromatography. There is no reason why a hydrated hypothetical Donnan membrane could not be built in our OT−CEC polymeric phases. Moreover, we did not state that “for column I, the bonded phase was only constructed of a molecular layer of chitosan”, even though we think a molecular layer of chitosan might also build a Donnan membrane. Instead, we stated a conclusion that column I and II phases were superior in the resolution and the analysis time to the phase simply bonded with a molecular layer of chitosan. In addition, the neutral marker was DMSO and had been stated in section 2.4.

*Graphical Abstract

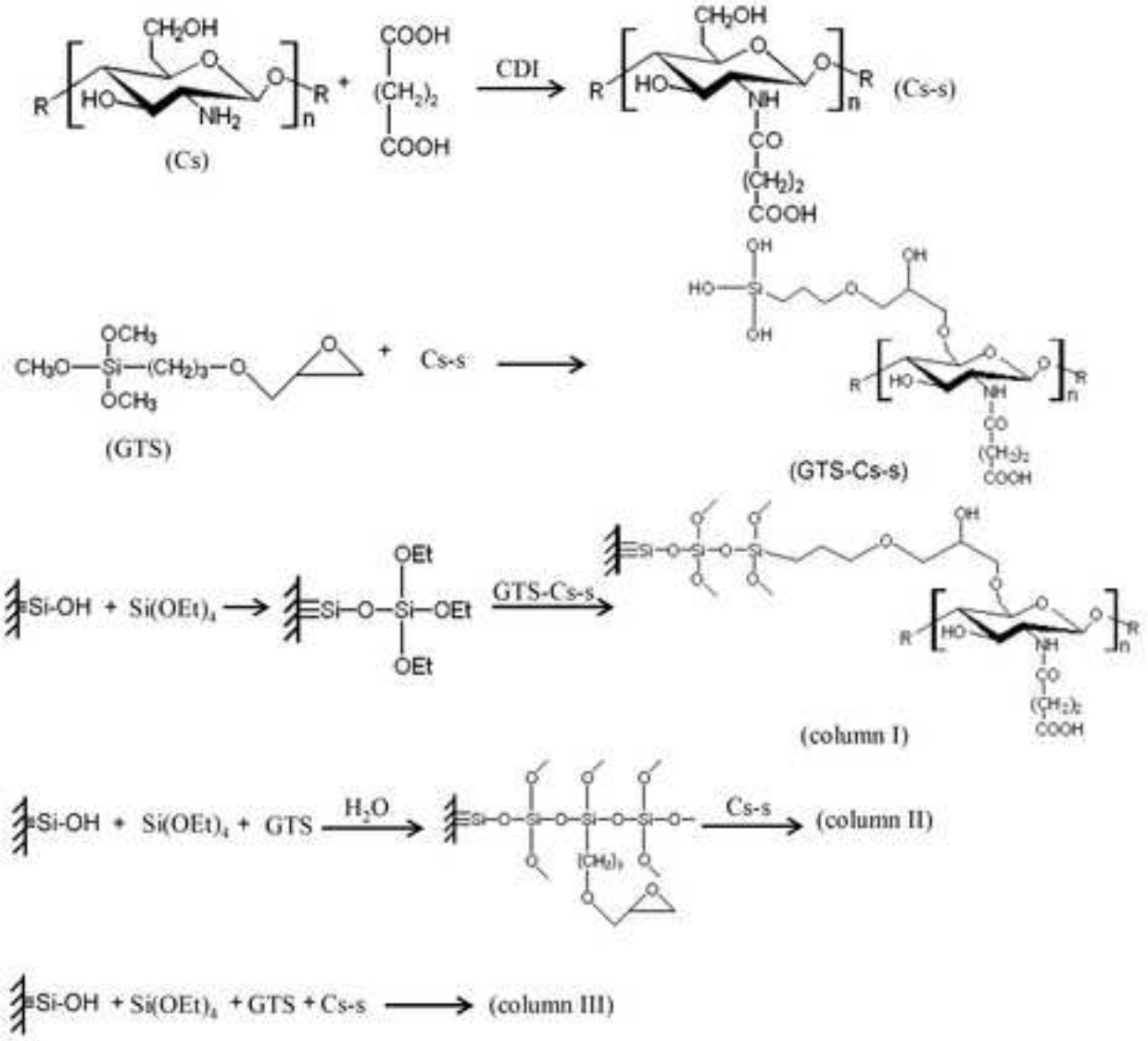

***Highlights**

1. Sequence in synthetic steps determines the chitosan loading in the sol-gel phases.
2. Chitosan moieties bearing carboxylic acid groups dominate the EOF.
3. High loading of the chitosan chiral selector caused the high k'' and α values.
4. Consider the hydrophobicity of the sol-gel phases in the chiral CEC separations.
5. Some sol-gel phases were superior in resolution and time to the monolayered phase.

*Underlined Revision

ACA-11-2023-Rev.Highlighted

Immobilization of chitosan in sol-gel phases for chiral open-tubular capillary electrochromatography

Jian-Lian Chen*, Hong-Jie Syu

School of Pharmacy, China Medical University, No. 91 Hsueh-Shih Road, Taichung 40402, Taiwan

Tel: (886) 4-2205-3366. Fax: (886) 4-2203-1075.

E-mail address: cjl@mail.cmu.edu.tw (J.-L. Chen).

Abstract:

Three different approaches for immobilizing cross-linked chitosan molecules (CS-s) in sol-gel phases to form chiral OT-CEC capillaries were comparatively investigated in this study. To synthesize column I, a bare capillary was first silanized with triethoxysilane (TEOS) and then reacted with the reaction product of 3-glycidyloxypropyltrimethoxysilane (GTS) and CS-s. Column II was prepared by the silanization of a bare capillary with a mixture of TEOS and GTS silanes followed by reaction with CS-s. To obtain column III, all the reagents, including TEOS, GTS, and CS-s were reacted together in a bare capillary. The SEM images showed that the column I phase consisted of two distinct layers, GTS and TEOS sol-gel films, while column II and III phases were homogeneous phases. By elemental analysis, the chitosan contents of the columns were found to decrease in the order column I > II > III, which corresponded to the order of the electroosmotic mobility values obtained from the measurements of the electroosmotic flow in the columns. The retention factor and the selectivity for the chiral separation of phenylglycine enantiomers in the optimized Tris running buffer (100 mM, pH 7.5) also followed this decreasing order. Besides the strength of the interaction with the immobilized functional chitosan, the ~~phase~~ hydrophobicity of the column affected the resolution of enantiomeric samples. The hydrophilic alanine sample could only be resolved by column III, but the hydrophobic tryptophan and catechin enantiomers were better separated by columns I and II. A reverse-phase mechanism has been found in the separations. Furthermore, the resolution and analysis time of column I and II phases were superior to the phase simply bonded with molecular chitosan.

Keywords: Capillary electrochromatography; Chiral stationary phase; Chitosan; Open-tubular; Sol-gel

Comment [c1]: Response 2 to Reviewer #3.

1. Introduction

The enantioseparation of chiral compounds is of continuous importance in pharmacodynamics research and the pharmaceutical industry. Direct chromatographic separation on a chiral stationary phase (CSP) is now the method of choice for stereoselective analysis, which is a challenging task in separation science [1,2]. Besides HPLC, capillary electrochromatography (CEC) is well-suited to the discovery of new CSPs using appropriate column formats developed using either particulate-packed, monolithic, or open-tubular (OT) columns, and many successful implementations have been reviewed [3−6].

Among the column technologies, an OT column is a relatively straightforward approach that does not require the arduous fabrication of frits, which are necessary in packed column construction, or the precise blending of monomer reagents with suitable porogens, as shown in the cases of monolithic fabrication. Although the OT column has low phase ratios, some chemical bonding strategies, such as the stepwise bonding of avidin or bovine serum albumin (BSA) proteins [7−9], molecularly imprinted polymer [10−12], and sol-gel coating with β–cyclodextrin or calixarene [7,13−15], have been adopted. In general, using macromolecules with plenty of recognition sites and/or using polymerized chiral selectors can increase the ~~chirality~~ chiral selectivity of the OT phase.

Comment [c2]: Response 3 to Reviewer #3.

Chitosan (CS, a functional linear polysaccharide) and its derivatives have been successfully immobilized in an HPLC/CSP system [16−18]. With regard to OT-CEC, chitosan with intrinsic basic properties has mainly been physically adsorbed on the bare capillaries, except for the carboxymethylchitosan covalently modified capillary, to separate bioactive molecules [19−21]. For the chiral separations using chitosan as a fixed chiral selector of CSP, a CEC monolith, which was composed of sol–gel/organic hybrid materials with the chiral selectivities of chitosan and BSA [22], was the only example aside from our recent studies [23,24]. In our previous study, an OT-CEC column was designed to have the nano-sized chitosan copolymerize with methacrylamide and exhibited promising chiral

separations of tryptophan, catechin, and α-tocopherol [23]. In another study, chitosan units were cross-linked in monolayered OT-CEC phases to increase the enantiomeric resolutions of tryptophan and catechin [24]. However, until now, chitosan molecules have not been incorporated in a sol-gel OT-CEC phase.

In this study, three OT-CEC columns with in situ polymerized or post-modified cross-linked chitosan molecules in sol-gel phases were fabricated and compared with regard to their SEM images, elemental analysis data, electroosmotic flow measurements, and enantiomeric resolutions. The difference in mechanism between the sol-gel capillaries was further discussed based on the electrochromatographic parameters for the enantioseparation of samples with different hydrophobicities, such as the amino acids, including phenylglycine, tryptophan, and alanine, as well as polyphenolic catechin.

2. Experimental

2.1. Materials

Most chemicals were of analytical or chromatographic grades. Chitosan (CS; from shrimp shells, practical grade, ≥ 75% deacetylated), 3-glycidyloxypropyltrimethoxysilane (GTS), triethoxysilane (TEOS), sodium tetraborate, phosphoric acid, sodium dihydrogenphosphate, hydrochloric acid, acetonitrile (ACN), and dimethylsulfoxide (DMSO) were purchased from Sigma–Aldrich (Milwaukee, WI, USA). Boric acid, acetic acid, ammonium carbonate, methanol (MeOH), 1,4-dioxane, and potassium acetate were obtained from Panreac (Barcelona, Spain). Sodium hydroxide, succinic acid, disodium hydrogenphosphate, trisodium phosphate, citric acid, sodium dihydrogen citrate, disodium hydrogen citrate, and trisodium citrate were supplied by Merck (Garmstadt, Germany). Acetone and sodium acetate were obtained from J.T. Baker (Phillipsburg, NJ, USA). Tris(hydroxymethyl)aminomethane (Tris) was obtained from TEDIA (Fairfield, OH, USA). The chemical 1-[3-(dimethylamino)propyl]-3-ethylcarbodiimide methiodide (CDI) was obtained from Acros

(Thermo Fisher Scientific, Geel, Belgium).

The enantiomeric samples, which include phenylglycine (PG), tryptophan (Trp), alanine (Ala), and catechins, (+)-(2R,3S)- and (−)-(2S,3R)-2-(3,4-dihydroxyphenyl)-3,4-dihydro-1(2H)-benzopyran-3,5,7-triol (their structures are shown in Fig. 1) were purchased from Sigma–Aldrich (Milwaukee, WI, USA). Sample concentrations were 1.0 mg/mL (Trp in H_2O; PG and Ala in MeOH) and 25 μg/mL (catechins in MeOH). Purified water (18 MΩ cm) from a Milli-Q water purification system (Millipore, Bedford, MA, USA) was used to prepare samples and buffer solutions.

2.2. Instrumentation

The laboratory-built electrophoresis apparatus was consisted of a ± 30 kV high-voltage power supply (TriSep TM-2100, Unimicro Technologies, CA, USA) and a UV-Vis detector (LCD 2083.2 CE, ECOM, Prague, Czech). Electrochromatograms were recorded using a Peak-ABC Chromatography Data Handling System (Kingtech Scientific, Taiwan). Elemental analyses were performed on an elemental carbon-hydrogen-nitrogen analyzer (elementar vario EL III, Hanau, Germany). A field-emission scanning electron microscope (Joel JSM-6700F, Japan) acquired the SEM images at an accelerating voltage of 3.0 kV.

2.3. Preparation of capillary columns

The preparation of the GTS-CS-s capillary without sol-gel layer but direct attachment of the epoxy silane and subsequent bonding of CS has been described previously [24]. The three approaches to preparing the sol-gel phases and the immobilization of chitosan are illustrated in Fig. 2.

2.3.1. Preparation of the TEOS+GTS/CS-s capillary (column I)

A new, bare capillary column, 70 cm, (Polymicro Technologies, Phoenix, AZ, USA) with a 375 μm O.D. x 75 μm I.D. was treated with 1.0 M NaOH and successively washed with pure water, 0.1 M HCl, pure water, and then acetone. The clean, bare capillary was filled with a TEOS solution (1.0 M in dioxane) and then kept in an oven for 1.5 h at 90°C to

undergo the silanization. After cooling to room temperature, the silanized capillary was ready for the following sol-gel reaction.

A 10 mL CS-s solution was prepared by dissolving succinic acid (8 mg) in water and then adjusting the solution pH to 6.5 with 0.1 M sodium hydroxide solution. After the addition of the CDI (40 mg) condensation agent, the alkaline mixture was stirred at 4°C for 30 min and subsequently mixed with chitosan (10 mg) at room temperature. The prepared CS-s solution (1 mL) was then added to the sol-gel precursor, GTS (100 μL), and reacted with the epoxide ring of GTS under ultrasonic agitation for 1 h. As soon as the sonication ceased, the sol-gel solution containing modified GTS silane was placed into the silanized capillary, and then the capillary was heated in a GC oven with a three-stage temperature program, including an initial temperature of 30^{o}C, an intermediate temperature of 100^{o}C (holding 30 min), and a final temperature of 150^{o}C (held for 4 h) at rate of increase of 2^{o}C/min. After the heating ended, the capillary was cooled to room temperature and was washed sequentially with MeOH and acetone for 30 min to complete the synthesis of the designated column I.

2.3.2. Preparation of TEOS/GTS+CS-s capillary (column II)

A mixture of TEOS (80 μL), GTS silanes (100 μL), and H_2O (9 μL) was used as the sol-gel solution to coat the capillary wall surface with a silica layer with epoxide-ring functionality that the CS-s molecules could be attached to. The sol-gel mixture was placed into a bare capillary and then heated in a GC oven using the same three-stage temperature program as described in section 2.3.1. After cooling the capillary to room temperature, the CS-s solution was completely filled in the capillary, which was then sonicated for 1 h and washed sequentially with MeOH and acetone for 30 min to complete the synthesis of the designated column II.

2.3.2. Preparation of TEOS/GTS/CS-s capillary (column III)

A mixture of TEOS (80 μL), GTS silanes (100 μL), and CS-s solution (1 mL) was sonicated for 1 h before placing it into a bare capillary. After heating in a GC oven using the same three-stage temperature program as described in section 2.3.1, the capillary was washed sequentially with MeOH and acetone for 30 min to complete the synthesis of the designated column III.

2.4. CEC conditions

Most experiments were conducted using common CZE buffers, including Tris, acetate, citrate, phosphate, ammonium carbonate, and borate buffers within a pH range of 5.5 to 11.5 and an ionic concentration range of 10 to 300 mM. ACN and MeOH were added to the buffers as organic modifiers. All prepared buffer solutions for CEC analyses were filtered through a 0.45 μm cellulose ester membrane (Adventec MFS, Pleasanton, CA, USA). DMSO was used as the neutral marker. The studied capillary was sequentially washed with methanol, water, and running buffer between each analysis run. Prior to sample injection, a working voltage was applied for 5 min to condition the charge distribution in the column. The prepared test samples were introduced by siphoning using a height difference. The samples were detected by UV light absorption measurements at 195 nm for alanine, 280 nm for catechin, and 214 nm for DMSO, phenylglycine, and tryptophan.

3. Results and discussion

3.1. Characterization of the sol-gel phases

3.1.1. SEM image and elementary analysis

The GTS-CS-s powder and the cross-sections of columns I, II, and III were observed by SEM, the images of which are shown in Fig. 3. The surface morphology of GTS-CS-s powder, which was obtained after heating the mixture of CS-s and GTS solution in a beaker, is shown in Fig. 3(A) and looks similar to the texture of the material coated on the upper layer of the modified phase in column I, as shown in Fig. 3(B). There were two apparently different

coatings in column I, where the GTS-CS-s sol reagent was coated on the first sol-gel layer, which was made of TEOS of approximately 5 μm thickness, and formed a second layer with a thickness of approximately 4 μm. The formed GTS-CS-s layer shown in the central part of the Fig. 3(B) image was relatively thick and the thick layer seems to have been caused by capillary cutting before SEM scanning. By contrast, the cross-sectional morphology of the coatings shown in Fig. 3(C) and 3(D), respectively, for columns II and III indicates the "hardness" of the phase composite of the TEOS and GTS sol reagent mixture and no damage to the integral phases during the cutting of the capillaries.

The difference in the morphology of columns II and III determined by SEM is small, but the difference in nitrogen content obtained by elemental analysis (EA) is significant, 1.82% (±0.03, n=5) vs. 1.14% (±0.02, n=5) for column II and III, respectively. As compared with column II and III, column I had the highest nitrogen percentage, 2.64% (±0.03, n=5). Here, the amount of chitosan loaded into these columns correlated with the nitrogen ratio and varied with different synthetic approaches. A comparison between the EA data of columns II and III revealed that the silanization and epoxide-ring opening reaction must occur stepwise, rather than simultaneously, to increase chitosan loading. Furthermore, if a high chitosan loading is intended, a comparison between columns I and II showed that a GTS reagent must undergo the epoxide-ring opening reaction with chitosan before rather than after its silanization with TEOS. In any event, very few nitrogen atoms, 0.12% (±0.04, n=5), were found in the GTS-CS-s capillary, whose bonded phase was only constructed of a molecular layer of chitosan.

3.1.2. Measurements of EOF for the sol-gel modified phases

To determine the EOF magnitude that contributed to solute migration in the CEC and to examine some of the chemical properties of the modified capillaries, the EOF driven by the capillaries under buffers with different pHs was characterized before the CS-immobilized capillaries were utilized for chiral analyses. The curves shown in Fig. 4 illustrate the

dependence of μ_{eo} on the pH of the phosphate buffer for the bare fused-silica capillary, the sol-gel capillaries, including columns I, II, and III, and the previously reported GTS-CS-s capillary.

As shown in Fig. 4, the curve pattern of the three sol-gel capillaries reached a plateau at higher pH levels and was dissimilar to that of the bare capillary, where the μ_{eo} values simply increased with increasing buffer pH. Accordingly, the effect of the residual silanol groups on the surface charges of the modified capillaries could be neglected as the chitosan macromolecules attached to the GTS silane coupling agents might shield most of the silanols. Here, the sheltered silanols could not affect the μ_{eo} values, but some of the chitosan moieties bearing carboxylic acid groups derived from succinic acid dominate the EOF. Succinic acid is characterized by the dicarboxylic acid moiety, which could partly act as a bridging agent to cross-link the chitosan units through amidation. The cross-linking reaction enriched the bonded chitosan units' blanketing the capillary wall surface and consequently enhancing the shielding effect.

The plateau curve at higher pH levels also occurred with the GTS-CS-s capillary. If the surface charge on the Cs-s-modified capillary wall was only due to the carboxylate groups of the CS-s molecules, the dissociation of the carboxylic acids would mainly determine the zeta potential or the electroosmotic mobilities (μ_{eo}) of the capillaries. As a result, a further examination of the curve pattern in Fig. 4 revealed that the carboxylic acids either in the GTS-CS-s phase or the sol-gel phases would be dissociated within the pH range between 4.5 and 7.5. The range correlated to the $p\mathrm{Ka}_2$ (5.2) of succinic acid at $\mu = 0.1$ [25]. However, the μ_{eo} values obtained at pH values higher than 8.0 in the CS-s-modified capillaries were somewhat diverse. Here, column II had higher μ_{eo} values than column III. Because the EA data showed that the CS-s content in column II was higher than that in column III, the surface density of succinate ligands on the column II phase would be higher than that on the column III phase. The column II and III phases were similarly created in the TEOS-formed silica

matrices, which could not contribute to an increase in zeta potential, but could reduce the μ_{eo} value. By contrast, the outermost surface layer of column I was simply constructed from the reaction ~~product~~ mixture of CS-s molecules and GTS silane without involvement of the TEOS silane, and therefore had higher μ_{eo} values than columns II and III. Besides, the μ_{eo} values of the GTS-CS-s capillary were close to that of column I, as they both have similar surface chemistry.

Comment [c3]: Response 1 to Reviewer #3.

The reproducibility of the capillary fabrication was evaluated using the μ_{eo} values measured at pH 7.6 for five runs of the sol-gel capillaries. The RSD values were 4.4±0.6%, 3.4±0.4%, and 4.0±0.4%, respectively, for three replicate capillaries, columns I, II, and III. At the 95% confidence level, no significant differences between the replicate columns were observed by the Student's *t*-test.

3.2. Enantiomeric separation of amino acids

3.2.1. Phenylglycine

Phenylglycine (PG) enantiomers were used as chiral probes to assess the CEC enantioselectivity of the modified sol-gel capillaries, columns I, II, and III. After testing several types of buffers (described in section 2.4), the best peak shape and resolution of the PG racemate were achieved using a Tris buffer system (100 mM, pH 7.5) and are shown in Fig. 5. As compared with the electrochromatograms in Fig. 5, the longest migration times of the PG solutes were found in column I, although the cathodic EOF of column I was higher than those of columns II and III, as shown in Fig. 4. There may be a stronger chromatographic retention between the column I phase and the PG solutes.

Differentiating between the electrophoretic and chromatographic contributions to the CEC separation is essential, particularly in this study, which focuses on the chiral selectivity induced by the fixed chitosan molecules. Adopting the definition formulated by Rathore and Horváth, measurements of electrophoretic migration and chromatographic retention in CEC can be described by a velocity factor (k_e'') and a retention factor (k''), respectively [26,27];

these terms are expressed in equations (1) and (2):

$$k_e'' = \frac{\mu_{ep}}{\mu_{eo2}} \quad (1)$$

$$k'' = \frac{\left[t_{M2} \times \left(1 + k_e'' \right) - t_{02} \right]}{t_{02}} \quad (2)$$

where μ_{ep} and μ_{eo2} are the electrophoretic and electroosmotic mobilities. These mobilities can be obtained from open-tubular CE experiments on a bare capillary (column 1) and from the CEC experiments on the CS-immobilized capillary (column 2), respectively, as follows:

$$\mu_{ep} = \frac{L_1 \times L_{d1}}{V_1} \times \left(\frac{1}{t_{M1}} - \frac{1}{t_{01}} \right) \quad (3)$$

$$\mu_{eo2} = \frac{L_2 \times L_{d2}}{t_{02} \times V_2} \quad (4)$$

where L is the total column length, L_d is the distance between the inlet and the detection point, V is the applied voltage, t_M is the migration time of the solute, and t_0 is the migration time of the neutral marker. The electrochromatographic parameters for the PGs separated under the conditions of Fig. 5 are summarized in Table 1. Here, the pI (6.56 at μ= 0.1) of PG is lower than the pH (7.5) of Tris running buffer [28], leading to the electrophoretic movement of PGs toward the anode and to negative k_e'' values. Moreover, the k_e'' values of the DL solutes in all of the columns were identical and indicated that the electrophoretic action did not contribute to the enantioseparation. By contrast, chromatographic selectivity due to the different k'' values of the DL solutes contributed to the enantioseparation. The negative k'' values are most likely to arise from the repulsive interaction between the negatively charged PGs and ionized succinate groups on the column phases. In addition, the high loading of the chitosan chiral selector would be responsible for the higher α and N values observed in the column I phase than those in the column II and III phases.

3.2.2. Tryptophan

Tryptophan (Trp) is more hydrophobic than PG [29]. As shown in Fig. 6, the optimal conditions for the separation of Trp enantiomers varied with the types of columns and, evidently, different amounts of MeOH was required in the Tris running buffers. The addition of MeOH into the running buffers would be expected to affect the chiral selectivity between the enantiomeric solutes in the CEC capillaries; the presence of the organic modifier not only altered the electrophoretic and electroosmotic flows, but it was also of interest to the chromatographic partitioning between the solute molecules and the stationary phases.

As shown in Fig. 6(A), the Tris buffer (50 mM) used in column I reached a high level of pH 10.0 but no MeOH was required. At pH 10.0, Trp molecules, with pKa_1 (2.35) and pKa_2 (9.33) at $\mu = 0.1$ [25], will be dissociated into their anionic form. Accordingly, the repulsive interaction between the Trp anions and the negatively charged succinate groups on the column I phase would greatly affect the enantiomer selectivity as in the chiral separation of PGs in section 3.2.1. As compared with the optimal buffer used in column I, the buffer pH level used for column II was lowered to 9.5, and 20% (v/v) MeOH was added to the buffer. These changes would decrease the EOF magnitude and increase the proportion of neutral to ionized Trp molecules. As a consequence, the repulsion between ionic solutes and succinate groups would be reduced, and the retention between neutral solutes and the immobilized chitosan selector would be enhanced. This conversion also exchanged the migration order from L/D to D/L Trp, as shown in Fig. 6(C) and (D), where the Tris buffers were optimized at pH 9.0 with 50% MeOH and at pH 8.5 without MeOH, respectively. Furthermore, the increase in retention with increased MeOH percentage from 40 to 50% could be observed for column III, as shown in Fig. 7. If the MeOH percentage was over 50%, the retention would start to decrease as the reverse phase mechanism contributed significantly here.

3.2.3. Alanine

Alanine (Ala) is more hydrophilic than PG, and its acid dissociation constants are pKa_1

293 (2.35) and pKa_2 (9.33) at μ = 0.1 [25,29]. Although Tris buffers of various pH values and
294 MeOH ratios were tried in all of the modified sol-gel columns, only column III could achieve
295 a distinct separation of Ala enantiomers in the optimized conditions, as shown in Fig. 8. In
296 comparison with column III, the lack of resolution in columns I and II could be due to their
297 higher loading of chitosan or their higher hydrophobicity, which is not favorable for
298 interaction with the hydrophilic Ala.
299 In comparison with the phenyl substituent in PG and the indole substituent in Trp, the
300 methyl group in the Ala structure could only provide a little retention with CS-immobilized
301 phases. The plot of k'' versus MeOH percentage is also shown in Fig. 7 and is an inverted
302 U-curve, which was caused by a balance between an increasing ratio of neutral to ionized
303 forms of Ala solutes and an increasing amount of neutral Ala solutes partitioning in MeOH as
304 the MeOH percentage was increased.
305 *3.3. Chiral separation of (±)-catechin*
306 (+)-(2R,3S)- and (−)-(2S,3R)-catechins are a category of flavonoids and have different
307 bioavailability and bioactivity [30,31]. Their hydrophobicity is higher than that of the amino
308 acids and they have acid dissociation constants of 8.16 (pKa_1) and 9.2 (pKa_2) [32]. As shown
309 in Fig. 9, they could be separated in the CS-immobilized columns with Tris running buffers.
310 Of the sol-gel capillaries, columns I and II had a better resolution than the GTS-CS-s capillary.
311 Here, the high loading of the chitosan chiral selector and the hydrophobic characteristic in
312 columns I and II were favorable factors for the separation of (±)-catechins.
313 Although the optimal conditions in different columns differed from each other, the effect
314 of the addition of MeOH into Tris buffer on the retention factor was similar. As shown in Fig.
315 10, the retention factors decreased with the increasing percentage of MeOH modifier. This
316 suggests that the reverse phase mechanism determined the chromatographic retention during
317 the CEC separation. Moreover, the strength of the retention factor decreased as column I > II
318 > III at a given MeOH proportion, as did the amount of chitosan in the columns.

4. Conclusions

Three OT-CEC capillaries, columns I, II, and III, with different approaches of immobilizing chitosan chiral selectors in sol-gel phases were successfully characterized and applied to chiral separations in this study. In addition to observing the morphology of the studied OT-CEC sol-gel capillaries by SEM, the chitosan contents were measured by elemental analyses of the nitrogen percentage and the μ_{eo} values were obtained by EOF measurements. The nitrogen percentage and the μ_{eo} values decreased in the order of column I > II > III. In the same Tris buffer system, column I, which had the highest loading of chitosan, showed a higher retention factor and selectivity (α) for the enantiomeric separation of phenylglycine than columns II and III. By contrast, column III could resolve the hydrophilic alanine enantiomers but columns I and II could not. For the hydrophobic samples of tryptophan and catechin enantiomers, the MeOH percentage in the running buffer greatly affected the resolutions, and the reversed phase mechanism was found in the column phases. Here, column I and II phases were superior in the resolution and the analysis time to the phase simply bonded with a molecular layer of chitosan. Although the peak performances in some separations did not meet the practical utility requirement, the optimization of the coating thickness and sol-gel composition ratio in the capillaries will be the possible ways to overcome the disadvantages.

Acknowledgements

Support of this work by the National Science Council of Taiwan (NSC−98−2113−M−039−003−MY3) is gratefully acknowledged.

References

[1] T.J. Ward, B.A. Baker, Anal. Chem. 80 (2008) 4363–4372.

[2] M. Lämmerhofer, J. Chromatogr. A, 1217 (2010) 814–856.

[3] G. Gübitz, M.G. Schmid, J. Chromatogr. A 1204 (2008) 140–156.

[4] B. Preinerstorfer, M. Lämmerhofer, W. Lindner, Electrophoresis 30 (2009) 100–136.

[5] Z. Zhang, R. Wu, M. Wu, H. Zou, Electrophoresis 31 (2010) 1457–1466

[6] H. Lu, G. Chen, Anal. Methods, 3 (2011) 488–508.

[7] R. Dai, L. Tang, H. Li, Y. Deng, R. Fu, Z. Parveen, J. Appl. Polym. Sci. 106 (2007) 2041–2046.

[8] S.K. Wiedmer, T. Bo, M.-L. Riekkola, Anal. Biochem. 373 (2008) 26–33.

[9] J. Olsson, J.G. Blomberg, J. Chromatogr. B 875 (2008) 329–332.

[10] S.A. Zaidi, W.J. Cheong, Electrophoresis 30 (2009) 1603–1607.

[11] S.A. Zaidi, K.M. Han, D.G. Hwang, W.J. Cheong, Electrophoresis 31 (2010) 1019–1028.

[12] S.A. Zaidi, S.M. Lee, W.J. Cheong, J. Chromatogr. A 1218 (2011) 1291–1299.

[13] Y. Wang, Z. Zeng, N. Guan, J. Cheng, Electrophoresis, 22 (2001) 2167–2172.

[14] C.-Q. Shou, J.-F. Kang, N.-J. Song, Chin. J. Anal. Chem. 36 (2008) 297–300.

[15] K. Hu, Y. Tian, H. Yang, J. Zhang, J. Xie, B. Ye, Y. Wu, S. Zhang, J. Liq. Chromatogr. Relat. Technol. 32 (2009) 2627–2641.

[16] Y. Liu, H. Zou, J. Haginaka, J. Sep. Sci. 29 (2006) 1440–1446.

[17] S.-H. Son, J. Jegal, J. Appl. Polym. Sci. 106 (2007) 2989–2996.

[18] C. Yamoto, M. Fujisawa, M. Kamigaito, Y. Okamoto, Chirality 20 (2008) 288–294.

[19] X. Huang, Q. Wang, B. Huang, Talanta 69 (2006) 463–468.

[20] X. Fu, Y. Liu, W. Li, N. Pang, H. Nie, H. Liu, Z. Cai, Electrophoresis 30 (2009) 1783–1789.

[21] S. Zhou, J. Tan, Q. Chen, X. Lin, H. Lü, Z. Xie, J. Chromatogr. A 1217 (2010) 8346–8351.

[22] M. Kato, H. Saruwatari, K. Sakai-Kato, T. Toyo'oka, J. Chromatogr. A 1044 (2004) 267–270.
[23] J.-L. Chen, K.-H. Hsieh, Electrophoresis 32 (2011) 398–407.
[24] J.-L. Chen, Talanta, 85 (2011) 2330–2338.
[25] A.E. Martell, R.M. Smith (Eds.), Critical Stability Constants, Plenum Press, New York, 1989.
[26] A.S. Rathore, Cs. Horváth, J. Chromatogr. A 743 (1996) 231–246.
[27] A.S. Rathore, Cs. Horváth, Electrophoresis 23 (2002) 1211–1216.
[28] A.A. Mohamed, F.I. El-Dossoki, H.A. Gumaa, J. Chem. Eng. Data 55 (2010) 673–678.
[29] E.S.J. Rudolph, M. Zomerdijk, M. Ottens, L.A.M. van der Wielen, Ind. Eng. Chem. Res. 40 (2001) 398–406.
[30] J.L. Donovan, V. Crespy, M. Oliveira, K.A. Copper, B.B. Gibson, G. Williamson, Free Radic. Res. 40 (2006) 1029–1034.
[31] F. Nyfeler, U.K. Moser, P. Walter, Biochim. Biophys. Acta 763 (1983) 50–57.
[32] D.A. El-Hady, N.A. El-Maali, Talanta 76 (2008) 138–145.

Figure captions and legends

Figure 1. Chemical structures of the chiral samples.

Figure 2. Schemes to synthesize the CS-immobilized sol-gel capillaries.

Figure 3. SEM images of GTS-CS-s powder (A) and coatings on the inner wall of column I (B), column II (C), and column III (D).

Figure 4. Dependence of electroosmotic mobility on buffer pH in different columns. Columns: (▲) a bare fused-silica capillary; (Δ) the GTS-CS-s capillary; (●) column I; (♦) column II; and (■) column III. Conditions: BGE, phosphate buffer, 50 mM; neutral marker, DMSO; hydrostatic injection, 5 cm, 2 sec; applied voltage, 15 kV; detection, 214 nm. The (▲) and (Δ) data were obtained from [24].

Figure 5. Enantioseparations of (D/L)-PG in the CS-immobilized sol-gel capillaries. Columns: (A) column I (55 cm (50 cm) x 75 μm I.D.); (B) column II (60 cm (55 cm) x 75 μm I.D.); and (C) column III (41 cm (38 cm) x 75 μm I.D.). BGE: Tris buffer, 100 mM, pH 7.5. The applied voltage was 8 kV. Samples: hydrostatic injection of 15 cm for 10 sec and detection at 214 nm. Peaks correspond to (1) L-PG, and (2) D-PG.

Figure 6. Enantioseparations of (D/L)-Trp in the CS-immobilized sol-gel capillaries. (A) column I (60 cm (55 cm) x 75 μm I.D.); (B) column II (60 cm (55 cm) x 75 μm I.D.); (C) column III (44 cm (38 cm) x 75 μm I.D.); and (D) GTS-CS-s (60 cm (55 cm) x 75 μm I.D.). BGE: Tris buffer, 50mM, (A) pH 10.0; (B) pH 9.5 with 20% MeOH; (C) pH 9.0 with 50% MeOH; and (D) pH 8.5. The applied voltage was 10 kV except for (D), which was 15 kV. Samples: hydrostatic injection of 15 cm for 10 sec and detection at 214 nm. Peaks correspond to (1) L-Trp, and (2) D-Trp.

Figure 7. Effect of the addition of MeOH into the Tris buffer on the retention factor (k'') of (D/L)-Trp and (D/L)-Ala in the column III. (◊) and (■) represent the k'' values of (*d*)-Trp and (*l*)-Trp, respectively, observed under the conditions in Fig. 6(C). (○) and (▲) represent the k'' values of D-Ala and L-Ala, respectively, observed under the conditions in Fig. 8.

Figure 8. Enantioseparations of (D/L)-Ala in column III (44 cm (39 cm) x 75 μm I.D.). BGE: Tris buffer, 50 mM, pH 10.5. The applied voltage was 15 kV. Samples: hydrostatic injection of 15 cm for 10 sec and detection at 195 nm. Peaks correspond to (S) MeOH solvent, (1) D-Ala, and (2) L-Ala.

Figure 9. Enantioseparations of (±)-catechins in the CS-immobilized sol-gel and GTS-CS-s capillaries. (A) column I (60 cm (55 cm) x 75 μm I.D.); BGE: Tris (pH 8.5, 50 mM) with MeOH (50%, v/v); 20 kV applied voltage; (B) column II (60 cm (55 cm) x 75 μm I.D.); BGE: Tris (pH 9.5, 50 mM) with MeOH (70%, v/v); 15 kV applied voltage; (C) column III (45 cm (40 cm) x 75 μm I.D.); BGE: Tris (pH 9.5, 50 mM) with MeOH (40%, v/v); 15 kV applied voltage; (D) GTS-CS-s (65 cm (60 cm) x 75 μm I.D.); BGE: Tris (pH 8.5, 100 mM) with MeOH (60%, v/v); 15 kV applied voltage. Samples: hydrostatic injection of 15 cm for 10 sec and detection at 280 nm. Peaks correspond to (S) MeOH solvent, (1) (–)-catechin, and (2) (+)-catechin.

Figure 10. Effect of the addition of MeOH into the Tris buffer on the retention factor (k'') of (±)-catechins in the CS-immobilized sol-gel capillaries. (♦)/(◊), (▲)/(Δ), and (■)/(□) were observed under the conditions in Fig. 9(A), 9(B), and 9(C), respectively. Black-filled symbols, (♦), (▲), and (■), and white-filled symbols, (◊), (Δ), and (□), represent the k'' values of (–)- and (+)-catechin, respectively.

Immobilization of chitosan in sol-gel phases for chiral open-tubular capillary electrochromatography

Jian-Lian Chen*, Hong-Jie Syu

School of Pharmacy, China Medical University, No. 91 Hsueh-Shih Road, Taichung 40402, Taiwan

Tel: (886) 4-2205-3366. Fax: (886) 4-2203-1075.

E-mail address: cjl@mail.cmu.edu.tw (J.-L. Chen).

Abstract:

Three different approaches for immobilizing cross-linked chitosan molecules (CS-s) in sol-gel phases to form chiral OT-CEC capillaries were comparatively investigated in this study. To synthesize column I, a bare capillary was first silanized with triethoxysilane (TEOS) and then reacted with the reaction product of 3-glycidyloxypropyltrimethoxysilane (GTS) and CS-s. Column II was prepared by the silanization of a bare capillary with a mixture of TEOS and GTS silanes followed by reaction with CS-s. To obtain column III, all the reagents, including TEOS, GTS, and CS-s were reacted together in a bare capillary. The SEM images showed that the column I phase consisted of two distinct layers, GTS and TEOS sol-gel films, while column II and III phases were homogeneous phases. By elemental analysis, the chitosan contents of the columns were found to decrease in the order column I > II > III, which corresponded to the order of the electroosmotic mobility values obtained from the measurements of the electroosmotic flow in the columns. The retention factor and the selectivity for the chiral separation of phenylglycine enantiomers in the optimized Tris running buffer (100 mM, pH 7.5) also followed this decreasing order. Besides the strength of the interaction with the immobilized functional chitosan, the hydrophobicity of the column affected the resolution of enantiomeric samples. The hydrophilic alanine sample could only be resolved by column III, but the hydrophobic tryptophan and catechin enantiomers were better separated by columns I and II. A reverse-phase mechanism has been found in the separations. Furthermore, the resolution and analysis time of column I and II phases were superior to the phase simply bonded with molecular chitosan.

Keywords: Capillary electrochromatography; Chiral stationary phase; Chitosan; Open-tubular; Sol-gel

1. Introduction

The enantioseparation of chiral compounds is of continuous importance in pharmacodynamics research and the pharmaceutical industry. Direct chromatographic separation on a chiral stationary phase (CSP) is now the method of choice for stereoselective analysis, which is a challenging task in separation science [1,2]. Besides HPLC, capillary electrochromatography (CEC) is well-suited to the discovery of new CSPs using appropriate column formats developed using either particulate-packed, monolithic, or open-tubular (OT) columns, and many successful implementations have been reviewed [3−6].

Among the column technologies, an OT column is a relatively straightforward approach that does not require the arduous fabrication of frits, which are necessary in packed column construction, or the precise blending of monomer reagents with suitable porogens, as shown in the cases of monolithic fabrication. Although the OT column has low phase ratios, some chemical bonding strategies, such as the stepwise bonding of avidin or bovine serum albumin (BSA) proteins [7−9], molecularly imprinted polymer [10−12], and sol-gel coating with β–cyclodextrin or calixarene [7,13−15], have been adopted. In general, using macromolecules with plenty of recognition sites and/or using polymerized chiral selectors can increase the chiral selectivity of the OT phase.

Chitosan (CS, a functional linear polysaccharide) and its derivatives have been successfully immobilized in an HPLC/CSP system [16−18]. With regard to OT-CEC, chitosan with intrinsic basic properties has mainly been physically adsorbed on the bare capillaries, except for the carboxymethylchitosan covalently modified capillary, to separate bioactive molecules [19−21]. For the chiral separations using chitosan as a fixed chiral selector of CSP, a CEC monolith, which was composed of sol–gel/organic hybrid materials with the chiral selectivities of chitosan and BSA [22], was the only example aside from our recent studies [23,24]. In our previous study, an OT-CEC column was designed to have the nano-sized chitosan copolymerize with methacrylamide and exhibited promising chiral

separations of tryptophan, catechin, and α-tocopherol [23]. In another study, chitosan units were cross-linked in monolayered OT-CEC phases to increase the enantiomeric resolutions of tryptophan and catechin [24]. However, until now, chitosan molecules have not been incorporated in a sol-gel OT-CEC phase.

In this study, three OT-CEC columns with in situ polymerized or post-modified cross-linked chitosan molecules in sol-gel phases were fabricated and compared with regard to their SEM images, elemental analysis data, electroosmotic flow measurements, and enantiomeric resolutions. The difference in mechanism between the sol-gel capillaries was further discussed based on the electrochromatographic parameters for the enantioseparation of samples with different hydrophobicities, such as the amino acids, including phenylglycine, tryptophan, and alanine, as well as polyphenolic catechin.

2. Experimental

2.1. Materials

Most chemicals were of analytical or chromatographic grades. Chitosan (CS; from shrimp shells, practical grade, ≥ 75% deacetylated), 3-glycidyloxypropyltrimethoxysilane (GTS), triethoxysilane (TEOS), sodium tetraborate, phosphoric acid, sodium dihydrogenphosphate, hydrochloric acid, acetonitrile (ACN), and dimethylsulfoxide (DMSO) were purchased from Sigma–Aldrich (Milwaukee, WI, USA). Boric acid, acetic acid, ammonium carbonate, methanol (MeOH), 1,4-dioxane, and potassium acetate were obtained from Panreac (Barcelona, Spain). Sodium hydroxide, succinic acid, disodium hydrogenphosphate, trisodium phosphate, citric acid, sodium dihydrogen citrate, disodium hydrogen citrate, and trisodium citrate were supplied by Merck (Garmstadt, Germany). Acetone and sodium acetate were obtained from J.T. Baker (Phillipsburg, NJ, USA). Tris(hydroxymethyl)aminomethane (Tris) was obtained from TEDIA (Fairfield, OH, USA). The chemical 1-[3-(dimethylamino)propyl]-3-ethylcarbodiimide methiodide (CDI) was obtained from Acros

(Thermo Fisher Scientific, Geel, Belgium).

The enantiomeric samples, which include phenylglycine (PG), tryptophan (Trp), alanine (Ala), and catechins, (+)-(2R,3S)- and (−)-(2S,3R)-2-(3,4-dihydroxyphenyl)-3,4-dihydro-1(2H)-benzopyran-3,5,7-triol (their structures are shown in Fig. 1) were purchased from Sigma–Aldrich (Milwaukee, WI, USA). Sample concentrations were 1.0 mg/mL (Trp in H_2O; PG and Ala in MeOH) and 25 μg/mL (catechins in MeOH). Purified water (18 MΩ cm) from a Milli-Q water purification system (Millipore, Bedford, MA, USA) was used to prepare samples and buffer solutions.

2.2. Instrumentation

The laboratory-built electrophoresis apparatus was consisted of a ± 30 kV high-voltage power supply (TriSep TM-2100, Unimicro Technologies, CA, USA) and a UV-Vis detector (LCD 2083.2 CE, ECOM, Prague, Czech). Electrochromatograms were recorded using a Peak-ABC Chromatography Data Handling System (Kingtech Scientific, Taiwan). Elemental analyses were performed on an elemental carbon-hydrogen-nitrogen analyzer (elementar vario EL III, Hanau, Germany). A field-emission scanning electron microscope (Joel JSM-6700F, Japan) acquired the SEM images at an accelerating voltage of 3.0 kV.

2.3. Preparation of capillary columns

The preparation of the GTS-CS-s capillary without sol-gel layer but direct attachment of the epoxy silane and subsequent bonding of CS has been described previously [24]. The three approaches to preparing the sol-gel phases and the immobilization of chitosan are illustrated in Fig. 2.

2.3.1. Preparation of the TEOS+GTS/CS-s capillary (column I)

A new, bare capillary column, 70 cm, (Polymicro Technologies, Phoenix, AZ, USA) with a 375 μm O.D. x 75 μm I.D. was treated with 1.0 M NaOH and successively washed with pure water, 0.1 M HCl, pure water, and then acetone. The clean, bare capillary was filled with a TEOS solution (1.0 M in dioxane) and then kept in an oven for 1.5 h at 90°C to

undergo the silanization. After cooling to room temperature, the silanized capillary was ready for the following sol-gel reaction.

A 10 mL CS-s solution was prepared by dissolving succinic acid (8 mg) in water and then adjusting the solution pH to 6.5 with 0.1 M sodium hydroxide solution. After the addition of the CDI (40 mg) condensation agent, the alkaline mixture was stirred at 4°C for 30 min and subsequently mixed with chitosan (10 mg) at room temperature. The prepared CS-s solution (1 mL) was then added to the sol-gel precursor, GTS (100 μL), and reacted with the epoxide ring of GTS under ultrasonic agitation for 1 h. As soon as the sonication ceased, the sol-gel solution containing modified GTS silane was placed into the silanized capillary, and then the capillary was heated in a GC oven with a three-stage temperature program, including an initial temperature of 30^{o}C, an intermediate temperature of 100^{o}C (holding 30 min), and a final temperature of 150^{o}C (held for 4 h) at rate of increase of 2^{o}C/min. After the heating ended, the capillary was cooled to room temperature and was washed sequentially with MeOH and acetone for 30 min to complete the synthesis of the designated column I.

2.3.2. Preparation of TEOS/GTS+CS-s capillary (column II)

A mixture of TEOS (80 μL), GTS silanes (100 μL), and H_2O (9 μL) was used as the sol-gel solution to coat the capillary wall surface with a silica layer with epoxide-ring functionality that the CS-s molecules could be attached to. The sol-gel mixture was placed into a bare capillary and then heated in a GC oven using the same three-stage temperature program as described in section 2.3.1. After cooling the capillary to room temperature, the CS-s solution was completely filled in the capillary, which was then sonicated for 1 h and washed sequentially with MeOH and acetone for 30 min to complete the synthesis of the designated column II.

2.3.2. Preparation of TEOS/GTS/CS-s capillary (column III)

A mixture of TEOS (80 μL), GTS silanes (100 μL), and CS-s solution (1 mL) was sonicated for 1 h before placing it into a bare capillary. After heating in a GC oven using the same three-stage temperature program as described in section 2.3.1, the capillary was washed sequentially with MeOH and acetone for 30 min to complete the synthesis of the designated column III.

2.4. CEC conditions

Most experiments were conducted using common CZE buffers, including Tris, acetate, citrate, phosphate, ammonium carbonate, and borate buffers within a pH range of 5.5 to 11.5 and an ionic concentration range of 10 to 300 mM. ACN and MeOH were added to the buffers as organic modifiers. All prepared buffer solutions for CEC analyses were filtered through a 0.45 μm cellulose ester membrane (Adventec MFS, Pleasanton, CA, USA). DMSO was used as the neutral marker. The studied capillary was sequentially washed with methanol, water, and running buffer between each analysis run. Prior to sample injection, a working voltage was applied for 5 min to condition the charge distribution in the column. The prepared test samples were introduced by siphoning using a height difference. The samples were detected by UV light absorption measurements at 195 nm for alanine, 280 nm for catechin, and 214 nm for DMSO, phenylglycine, and tryptophan.

3. Results and discussion

3.1. Characterization of the sol-gel phases

3.1.1. SEM image and elementary analysis

The GTS-CS-s powder and the cross-sections of columns I, II, and III were observed by SEM, the images of which are shown in Fig. 3. The surface morphology of GTS-CS-s powder, which was obtained after heating the mixture of CS-s and GTS solution in a beaker, is shown in Fig. 3(A) and looks similar to the texture of the material coated on the upper layer of the modified phase in column I, as shown in Fig. 3(B). There were two apparently different

coatings in column I, where the GTS-CS-s sol reagent was coated on the first sol-gel layer, which was made of TEOS of approximately 5 μm thickness, and formed a second layer with a thickness of approximately 4 μm. The formed GTS-CS-s layer shown in the central part of the Fig. 3(B) image was relatively thick and the thick layer seems to have been caused by capillary cutting before SEM scanning. By contrast, the cross-sectional morphology of the coatings shown in Fig. 3(C) and 3(D), respectively, for columns II and III indicates the "hardness" of the phase composite of the TEOS and GTS sol reagent mixture and no damage to the integral phases during the cutting of the capillaries.

The difference in the morphology of columns II and III determined by SEM is small, but the difference in nitrogen content obtained by elemental analysis (EA) is significant, 1.82% (±0.03, n=5) vs. 1.14% (±0.02, n=5) for column II and III, respectively. As compared with column II and III, column I had the highest nitrogen percentage, 2.64% (±0.03, n=5). Here, the amount of chitosan loaded into these columns correlated with the nitrogen ratio and varied with different synthetic approaches. A comparison between the EA data of columns II and III revealed that the silanization and epoxide-ring opening reaction must occur stepwise, rather than simultaneously, to increase chitosan loading. Furthermore, if a high chitosan loading is intended, a comparison between columns I and II showed that a GTS reagent must undergo the epoxide-ring opening reaction with chitosan before rather than after its silanization with TEOS. In any event, very few nitrogen atoms, 0.12% (±0.04, n=5), were found in the GTS-CS-s capillary, whose bonded phase was only constructed of a molecular layer of chitosan.

3.1.2. Measurements of EOF for the sol-gel modified phases

To determine the EOF magnitude that contributed to solute migration in the CEC and to examine some of the chemical properties of the modified capillaries, the EOF driven by the capillaries under buffers with different pHs was characterized before the CS-immobilized capillaries were utilized for chiral analyses. The curves shown in Fig. 4 illustrate the

dependence of μ_{eo} on the pH of the phosphate buffer for the bare fused-silica capillary, the sol-gel capillaries, including columns I, II, and III, and the previously reported GTS-CS-s capillary.

As shown in Fig. 4, the curve pattern of the three sol-gel capillaries reached a plateau at higher pH levels and was dissimilar to that of the bare capillary, where the μ_{eo} values simply increased with increasing buffer pH. Accordingly, the effect of the residual silanol groups on the surface charges of the modified capillaries could be neglected as the chitosan macromolecules attached to the GTS silane coupling agents might shield most of the silanols. Here, the sheltered silanols could not affect the μ_{eo} values, but some of the chitosan moieties bearing carboxylic acid groups derived from succinic acid dominate the EOF. Succinic acid is characterized by the dicarboxylic acid moiety, which could partly act as a bridging agent to cross-link the chitosan units through amidation. The cross-linking reaction enriched the bonded chitosan units' blanketing the capillary wall surface and consequently enhancing the shielding effect.

The plateau curve at higher pH levels also occurred with the GTS-CS-s capillary. If the surface charge on the Cs-s-modified capillary wall was only due to the carboxylate groups of the CS-s molecules, the dissociation of the carboxylic acids would mainly determine the zeta potential or the electroosmotic mobilities (μ_{eo}) of the capillaries. As a result, a further examination of the curve pattern in Fig. 4 revealed that the carboxylic acids either in the GTS-CS-s phase or the sol-gel phases would be dissociated within the pH range between 4.5 and 7.5. The range correlated to the $p\mathrm{Ka}_2$ (5.2) of succinic acid at $\mu = 0.1$ [25]. However, the μ_{eo} values obtained at pH values higher than 8.0 in the CS-s-modified capillaries were somewhat diverse. Here, column II had higher μ_{eo} values than column III. Because the EA data showed that the CS-s content in column II was higher than that in column III, the surface density of succinate ligands on the column II phase would be higher than that on the column III phase. The column II and III phases were similarly created in the TEOS-formed silica

matrices, which could not contribute to an increase in zeta potential, but could reduce the μ_{eo} value. By contrast, the outermost surface layer of column I was simply constructed from the reaction mixture of CS-s molecules and GTS silane without involvement of the TEOS silane, and therefore had higher μ_{eo} values than columns II and III. Besides, the μ_{eo} values of the GTS-CS-s capillary were close to that of column I, as they both have similar surface chemistry.

The reproducibility of the capillary fabrication was evaluated using the μ_{eo} values measured at pH 7.6 for five runs of the sol-gel capillaries. The RSD values were 4.4±0.6%, 3.4±0.4%, and 4.0±0.4%, respectively, for three replicate capillaries, columns I, II, and III. At the 95% confidence level, no significant differences between the replicate columns were observed by the Student's *t*-test.

3.2. Enantiomeric separation of amino acids

3.2.1. Phenylglycine

Phenylglycine (PG) enantiomers were used as chiral probes to assess the CEC enantioselectivity of the modified sol-gel capillaries, columns I, II, and III. After testing several types of buffers (described in section 2.4), the best peak shape and resolution of the PG racemate were achieved using a Tris buffer system (100 mM, pH 7.5) and are shown in Fig. 5. As compared with the electrochromatograms in Fig. 5, the longest migration times of the PG solutes were found in column I, although the cathodic EOF of column I was higher than those of columns II and III, as shown in Fig. 4. There may be a stronger chromatographic retention between the column I phase and the PG solutes.

Differentiating between the electrophoretic and chromatographic contributions to the CEC separation is essential, particularly in this study, which focuses on the chiral selectivity induced by the fixed chitosan molecules. Adopting the definition formulated by Rathore and Horváth, measurements of electrophoretic migration and chromatographic retention in CEC can be described by a velocity factor (k_e'') and a retention factor (k''), respectively [26,27];

these terms are expressed in equations (1) and (2):

$$k_e'' = \frac{\mu_{ep}}{\mu_{eo2}} \quad (1)$$

$$k'' = \frac{\left[t_{M2} \times \left(1 + k_e''\right) - t_{02}\right]}{t_{02}} \quad (2)$$

where μ_{ep} and μ_{eo2} are the electrophoretic and electroosmotic mobilities. These mobilities can be obtained from open-tubular CE experiments on a bare capillary (column 1) and from the CEC experiments on the CS-immobilized capillary (column 2), respectively, as follows:

$$\mu_{ep} = \frac{L_1 \times L_{d1}}{V_1} \times \left(\frac{1}{t_{M1}} - \frac{1}{t_{01}}\right) \quad (3)$$

$$\mu_{eo2} = \frac{L_2 \times L_{d2}}{t_{02} \times V_2} \quad (4)$$

where L is the total column length, L_d is the distance between the inlet and the detection point, V is the applied voltage, t_M is the migration time of the solute, and t_0 is the migration time of the neutral marker. The electrochromatographic parameters for the PGs separated under the conditions of Fig. 5 are summarized in Table 1. Here, the pI (6.56 at μ= 0.1) of PG is lower than the pH (7.5) of Tris running buffer [28], leading to the electrophoretic movement of PGs toward the anode and to negative k_e'' values. Moreover, the k_e'' values of the DL solutes in all of the columns were identical and indicated that the electrophoretic action did not contribute to the enantioseparation. By contrast, chromatographic selectivity due to the different k'' values of the DL solutes contributed to the enantioseparation. The negative k'' values are most likely to arise from the repulsive interaction between the negatively charged PGs and ionized succinate groups on the column phases. In addition, the high loading of the chitosan chiral selector would be responsible for the higher α and N values observed in the column I phase than those in the column II and III phases.

3.2.2. Tryptophan

Tryptophan (Trp) is more hydrophobic than PG [29]. As shown in Fig. 6, the optimal conditions for the separation of Trp enantiomers varied with the types of columns and, evidently, different amounts of MeOH was required in the Tris running buffers. The addition of MeOH into the running buffers would be expected to affect the chiral selectivity between the enantiomeric solutes in the CEC capillaries; the presence of the organic modifier not only altered the electrophoretic and electroosmotic flows, but it was also of interest to the chromatographic partitioning between the solute molecules and the stationary phases.

As shown in Fig. 6(A), the Tris buffer (50 mM) used in column I reached a high level of pH 10.0 but no MeOH was required. At pH 10.0, Trp molecules, with pKa_1 (2.35) and pKa_2 (9.33) at $\mu = 0.1$ [25], will be dissociated into their anionic form. Accordingly, the repulsive interaction between the Trp anions and the negatively charged succinate groups on the column I phase would greatly affect the enantiomer selectivity as in the chiral separation of PGs in section 3.2.1. As compared with the optimal buffer used in column I, the buffer pH level used for column II was lowered to 9.5, and 20% (v/v) MeOH was added to the buffer. These changes would decrease the EOF magnitude and increase the proportion of neutral to ionized Trp molecules. As a consequence, the repulsion between ionic solutes and succinate groups would be reduced, and the retention between neutral solutes and the immobilized chitosan selector would be enhanced. This conversion also exchanged the migration order from L/D to D/L Trp, as shown in Fig. 6(C) and (D), where the Tris buffers were optimized at pH 9.0 with 50% MeOH and at pH 8.5 without MeOH, respectively. Furthermore, the increase in retention with increased MeOH percentage from 40 to 50% could be observed for column III, as shown in Fig. 7. If the MeOH percentage was over 50%, the retention would start to decrease as the reverse phase mechanism contributed significantly here.

3.2.3. Alanine

Alanine (Ala) is more hydrophilic than PG, and its acid dissociation constants are pKa_1

(2.35) and pKa_2 (9.33) at $\mu = 0.1$ [25,29]. Although Tris buffers of various pH values and MeOH ratios were tried in all of the modified sol-gel columns, only column III could achieve a distinct separation of Ala enantiomers in the optimized conditions, as shown in Fig. 8. In comparison with column III, the lack of resolution in columns I and II could be due to their higher loading of chitosan or their higher hydrophobicity, which is not favorable for interaction with the hydrophilic Ala.

In comparison with the phenyl substituent in PG and the indole substituent in Trp, the methyl group in the Ala structure could only provide a little retention with CS-immobilized phases. The plot of k'' versus MeOH percentage is also shown in Fig. 7 and is an inverted U-curve, which was caused by a balance between an increasing ratio of neutral to ionized forms of Ala solutes and an increasing amount of neutral Ala solutes partitioning in MeOH as the MeOH percentage was increased.

3.3. Chiral separation of (±)-catechin

(+)-(2R,3S)- and (−)-(2S,3R)-catechins are a category of flavonoids and have different bioavailability and bioactivity [30,31]. Their hydrophobicity is higher than that of the amino acids and they have acid dissociation constants of 8.16 (pKa_1) and 9.2 (pKa_2) [32]. As shown in Fig. 9, they could be separated in the CS-immobilized columns with Tris running buffers. Of the sol-gel capillaries, columns I and II had a better resolution than the GTS-CS-s capillary. Here, the high loading of the chitosan chiral selector and the hydrophobic characteristic in columns I and II were favorable factors for the separation of (±)-catechins.

Although the optimal conditions in different columns differed from each other, the effect of the addition of MeOH into Tris buffer on the retention factor was similar. As shown in Fig. 10, the retention factors decreased with the increasing percentage of MeOH modifier. This suggests that the reverse phase mechanism determined the chromatographic retention during the CEC separation. Moreover, the strength of the retention factor decreased as column I > II > III at a given MeOH proportion, as did the amount of chitosan in the columns.

4. Conclusions

Three OT-CEC capillaries, columns I, II, and III, with different approaches of immobilizing chitosan chiral selectors in sol-gel phases were successfully characterized and applied to chiral separations in this study. In addition to observing the morphology of the studied OT-CEC sol-gel capillaries by SEM, the chitosan contents were measured by elemental analyses of the nitrogen percentage and the μ_{eo} values were obtained by EOF measurements. The nitrogen percentage and the μ_{eo} values decreased in the order of column I > II > III. In the same Tris buffer system, column I, which had the highest loading of chitosan, showed a higher retention factor and selectivity (α) for the enantiomeric separation of phenylglycine than columns II and III. By contrast, column III could resolve the hydrophilic alanine enantiomers but columns I and II could not. For the hydrophobic samples of tryptophan and catechin enantiomers, the MeOH percentage in the running buffer greatly affected the resolutions, and the reversed phase mechanism was found in the column phases. Here, column I and II phases were superior in the resolution and the analysis time to the phase simply bonded with a molecular layer of chitosan. Although the peak performances in some separations did not meet the practical utility requirement, the optimization of the coating thickness and sol-gel composition ratio in the capillaries will be the possible ways to overcome the disadvantages.

Acknowledgements

Support of this work by the National Science Council of Taiwan (NSC−98−2113−M−039−003−MY3) is gratefully acknowledged.

References

[1] T.J. Ward, B.A. Baker, Anal. Chem. 80 (2008) 4363–4372.

[2] M. Lämmerhofer, J. Chromatogr. A, 1217 (2010) 814–856.

[3] G. Gübitz, M.G. Schmid, J. Chromatogr. A 1204 (2008) 140–156.

[4] B. Preinerstorfer, M. Lämmerhofer, W. Lindner, Electrophoresis 30 (2009) 100–136.

[5] Z. Zhang, R. Wu, M. Wu, H. Zou, Electrophoresis 31 (2010) 1457–1466

[6] H. Lu, G. Chen, Anal. Methods, 3 (2011) 488–508.

[7] R. Dai, L. Tang, H. Li, Y. Deng, R. Fu, Z. Parveen, J. Appl. Polym. Sci. 106 (2007) 2041–2046.

[8] S.K. Wiedmer, T. Bo, M.-L. Riekkola, Anal. Biochem. 373 (2008) 26–33.

[9] J. Olsson, J.G. Blomberg, J. Chromatogr. B 875 (2008) 329–332.

[10] S.A. Zaidi, W.J. Cheong, Electrophoresis 30 (2009) 1603–1607.

[11] S.A. Zaidi, K.M. Han, D.G. Hwang, W.J. Cheong, Electrophoresis 31 (2010) 1019–1028.

[12] S.A. Zaidi, S.M. Lee, W.J. Cheong, J. Chromatogr. A 1218 (2011) 1291–1299.

[13] Y. Wang, Z. Zeng, N. Guan, J. Cheng, Electrophoresis, 22 (2001) 2167–2172.

[14] C.-Q. Shou, J.-F. Kang, N.-J. Song, Chin. J. Anal. Chem. 36 (2008) 297–300.

[15] K. Hu, Y. Tian, H. Yang, J. Zhang, J. Xie, B. Ye, Y. Wu, S. Zhang, J. Liq. Chromatogr. Relat. Technol. 32 (2009) 2627–2641.

[16] Y. Liu, H. Zou, J. Haginaka, J. Sep. Sci. 29 (2006) 1440–1446.

[17] S.-H. Son, J. Jegal, J. Appl. Polym. Sci. 106 (2007) 2989–2996.

[18] C. Yamoto, M. Fujisawa, M. Kamigaito, Y. Okamoto, Chirality 20 (2008) 288–294.

[19] X. Huang, Q. Wang, B. Huang, Talanta 69 (2006) 463–468.

[20] X. Fu, Y. Liu, W. Li, N. Pang, H. Nie, H. Liu, Z. Cai, Electrophoresis 30 (2009) 1783–1789.

[21] S. Zhou, J. Tan, Q. Chen, X. Lin, H. Lü, Z. Xie, J. Chromatogr. A 1217 (2010) 8346–8351.

[22] M. Kato, H. Saruwatari, K. Sakai-Kato, T. Toyo'oka, J. Chromatogr. A 1044 (2004) 267–270.

[23] J.-L. Chen, K.-H. Hsieh, Electrophoresis 32 (2011) 398–407.

[24] J.-L. Chen, Talanta, 85 (2011) 2330–2338.

[25] A.E. Martell, R.M. Smith (Eds.), Critical Stability Constants, Plenum Press, New York, 1989.

[26] A.S. Rathore, Cs. Horváth, J. Chromatogr. A 743 (1996) 231–246.

[27] A.S. Rathore, Cs. Horváth, Electrophoresis 23 (2002) 1211–1216.

[28] A.A. Mohamed, F.I. El-Dossoki, H.A. Gumaa, J. Chem. Eng. Data 55 (2010) 673–678.

[29] E.S.J. Rudolph, M. Zomerdijk, M. Ottens, L.A.M. van der Wielen, Ind. Eng. Chem. Res. 40 (2001) 398–406.

[30] J.L. Donovan, V. Crespy, M. Oliveira, K.A. Copper, B.B. Gibson, G. Williamson, Free Radic. Res. 40 (2006) 1029–1034.

[31] F. Nyfeler, U.K. Moser, P. Walter, Biochim. Biophys. Acta 763 (1983) 50–57.

[32] D.A. El-Hady, N.A. El-Maali, Talanta 76 (2008) 138–145.

Figure captions and legends

Figure 1. Chemical structures of the chiral samples.

Figure 2. Schemes to synthesize the CS-immobilized sol-gel capillaries.

Figure 3. SEM images of GTS-CS-s powder (A) and coatings on the inner wall of column I (B), column II (C), and column III (D).

Figure 4. Dependence of electroosmotic mobility on buffer pH in different columns. Columns: (▲) a bare fused-silica capillary; (Δ) the GTS-CS-s capillary; (●) column I; (♦) column II; and (■) column III. Conditions: BGE, phosphate buffer, 50 mM; neutral marker, DMSO; hydrostatic injection, 5 cm, 2 sec; applied voltage, 15 kV; detection, 214 nm. The (▲) and (Δ) data were obtained from [24].

Figure 5. Enantioseparations of (D/L)-PG in the CS-immobilized sol-gel capillaries. Columns: (A) column I (55 cm (50 cm) x 75 μm I.D.); (B) column II (60 cm (55 cm) x 75 μm I.D.); and (C) column III (41 cm (38 cm) x 75 μm I.D.). BGE: Tris buffer, 100 mM, pH 7.5. The applied voltage was 8 kV. Samples: hydrostatic injection of 15 cm for 10 sec and detection at 214 nm. Peaks correspond to (1) L-PG, and (2) D-PG.

Figure 6. Enantioseparations of (D/L)-Trp in the CS-immobilized sol-gel capillaries. (A) column I (60 cm (55 cm) x 75 μm I.D.); (B) column II (60 cm (55 cm) x 75 μm I.D.); (C) column III (44 cm (38 cm) x 75 μm I.D.); and (D) GTS-CS-s (60 cm (55 cm) x 75 μm I.D.). BGE: Tris buffer, 50mM, (A) pH 10.0; (B) pH 9.5 with 20% MeOH; (C) pH 9.0 with 50% MeOH; and (D) pH 8.5. The applied voltage was 10 kV except for (D), which was 15 kV. Samples: hydrostatic injection of 15 cm for 10 sec and detection at 214 nm. Peaks correspond to (1) L-Trp, and (2) D-Trp.

Figure 7. Effect of the addition of MeOH into the Tris buffer on the retention factor (k'') of (D/L)-Trp and (D/L)-Ala in the column III. (◊) and (■) represent the k'' values of (*d*)-Trp and (*l*)-Trp, respectively, observed under the conditions in Fig. 6(C). (○) and (▲) represent the k'' values of D-Ala and L-Ala, respectively, observed under the conditions in Fig. 8.

Figure 8. Enantioseparations of (D/L)-Ala in column III (44 cm (39 cm) x 75 μm I.D.). BGE: Tris buffer, 50 mM, pH 10.5. The applied voltage was 15 kV. Samples: hydrostatic injection of 15 cm for 10 sec and detection at 195 nm. Peaks correspond to (S) MeOH solvent, (1) D-Ala, and (2) L-Ala.

Figure 9. Enantioseparations of (±)-catechins in the CS-immobilized sol-gel and GTS-CS-s capillaries. (A) column I (60 cm (55 cm) x 75 μm I.D.); BGE: Tris (pH 8.5, 50 mM) with MeOH (50%, v/v); 20 kV applied voltage; (B) column II (60 cm (55 cm) x 75 μm I.D.); BGE: Tris (pH 9.5, 50 mM) with MeOH (70%, v/v); 15 kV applied voltage; (C) column III (45 cm (40 cm) x 75 μm I.D.); BGE: Tris (pH 9.5, 50 mM) with MeOH (40%, v/v); 15 kV applied voltage; (D) GTS-CS-s (65 cm (60 cm) x 75 μm I.D.); BGE: Tris (pH 8.5, 100 mM) with MeOH (60%, v/v); 15 kV applied voltage. Samples: hydrostatic injection of 15 cm for 10 sec and detection at 280 nm. Peaks correspond to (S) MeOH solvent, (1) (–)-catechin, and (2) (+)-catechin.

Figure 10. Effect of the addition of MeOH into the Tris buffer on the retention factor (k'') of (±)-catechins in the CS-immobilized sol-gel capillaries. (♦)/(◊), (▲)/(Δ), and (■)/(□) were observed under the conditions in Fig. 9(A), 9(B), and 9(C), respectively. Black-filled symbols, (♦), (▲), and (■), and white-filled symbols, (◊), (Δ), and (□), represent the k'' values of (–)- and (+)-catechin, respectively.

Table 1

Electrochromatographic parameters of the phenylglycine (PG) enantiomer separated in the sol-gel chitosan-immobilized columns with the Tris buffer (pH 7.5, 100 mM)*

Column	PG	t_{M2} (min)	k_e''	k''	α (k_L''/ k_D'')	N (×10^4)	Rs
I	L	23.413	-0.42	-0.23	1.28	2.7	3.6
	D	24.823	-0.42	-0.19		4.3	
II	L	19.173	-0.44	-0.45	1.10	1.5	2.4
	D	20.612	-0.44	-0.41		1.9	
III	L	11.561	-0.52	-0.54	1.08	1.2	2.3
	D	13.257	-0.52	-0.50		1.3	

* Other CEC conditions are the same as those shown in Fig .5.

Figure-1

Click here to download high resolution image

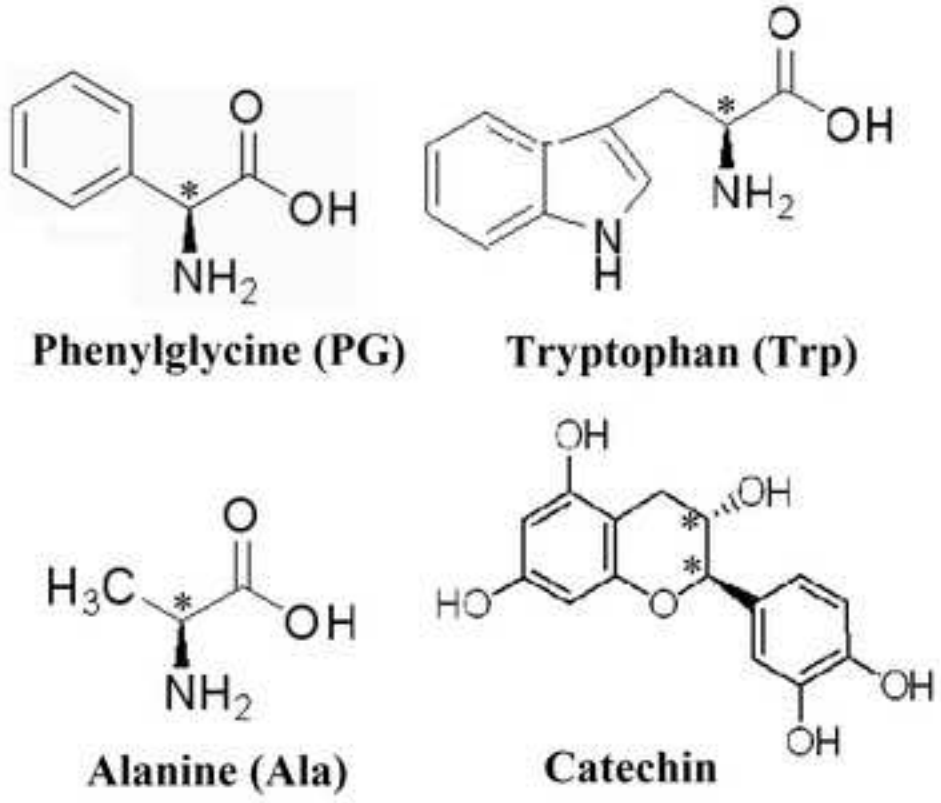

Figure-3

Click here to download high resolution image

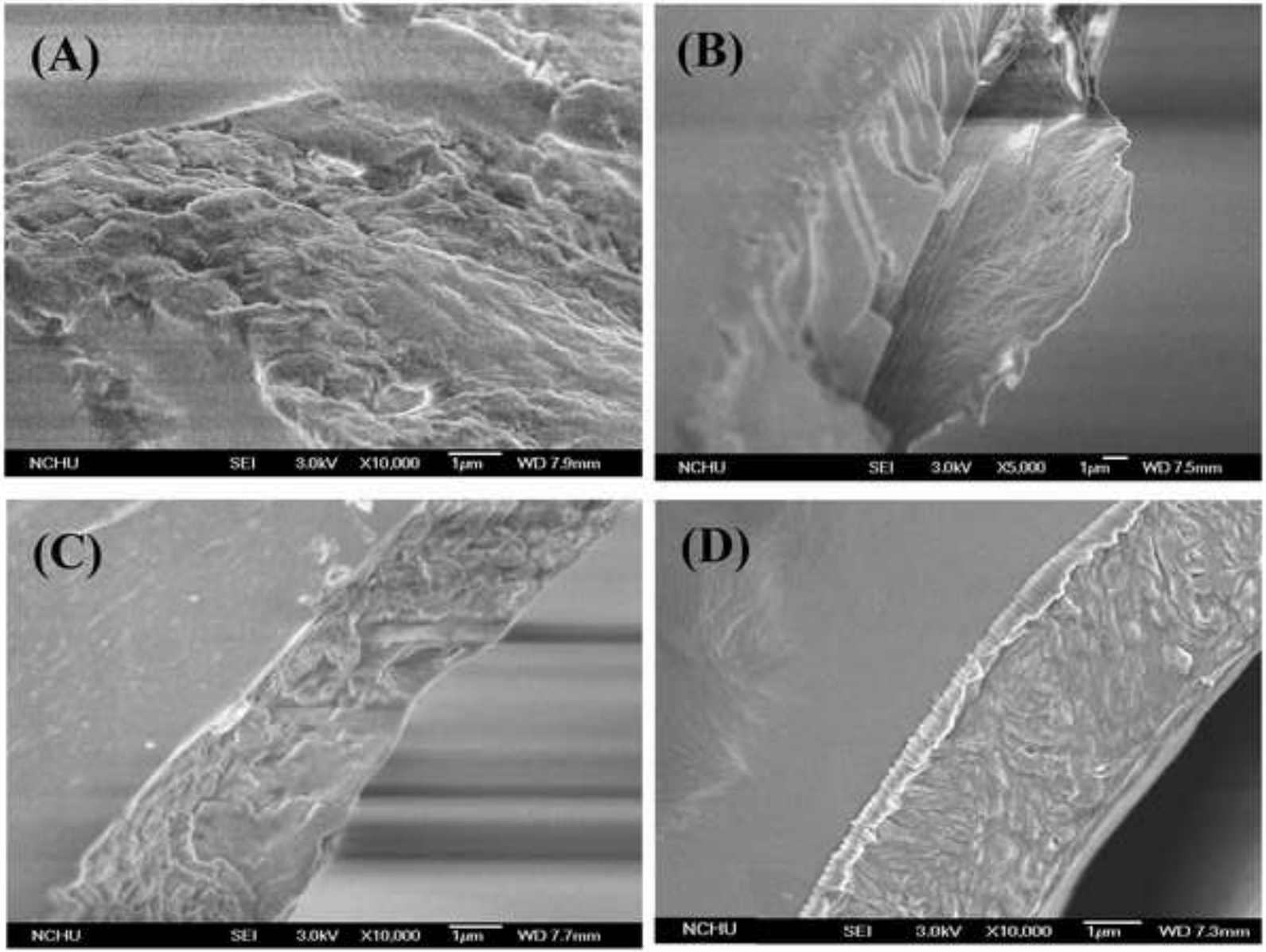

Figure-4

Click here to download high resolution image

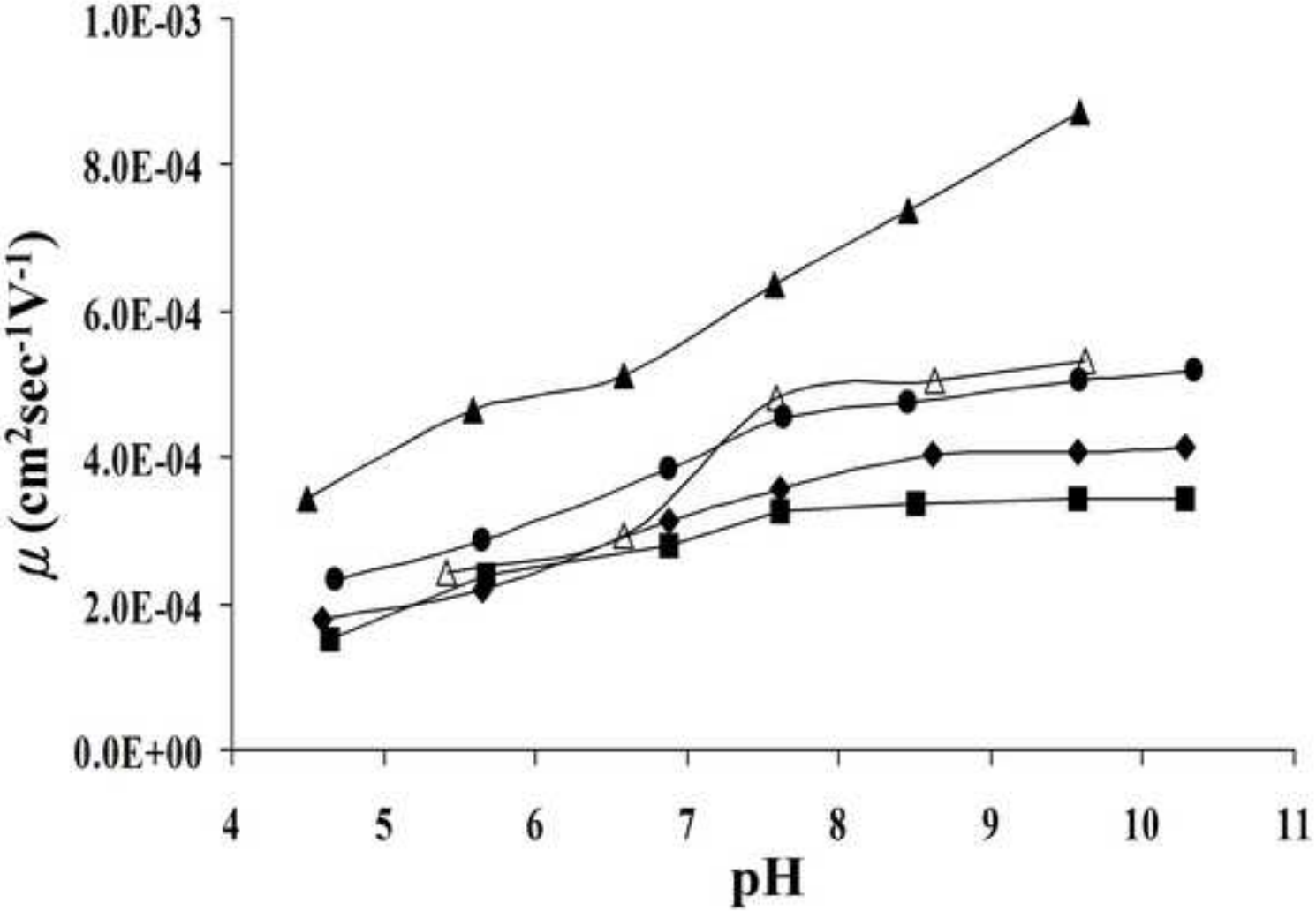

Figure-7

Click here to download high resolution image

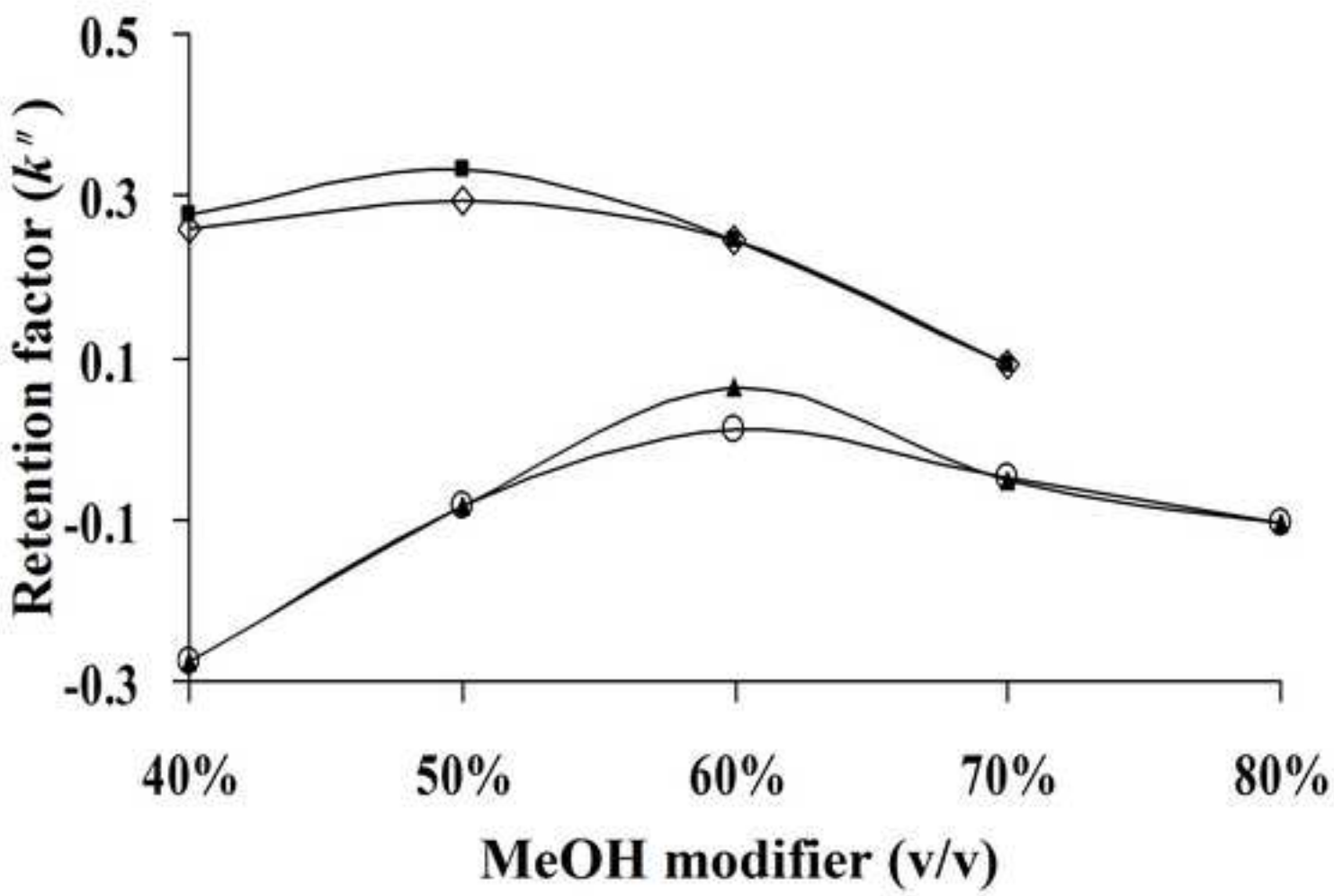

Figure-8

Click here to download high resolution image

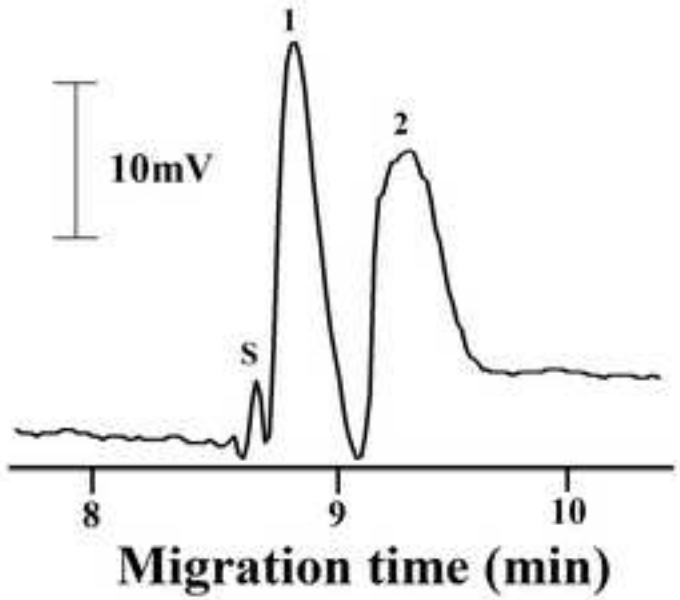

Figure-10

Click here to download high resolution image

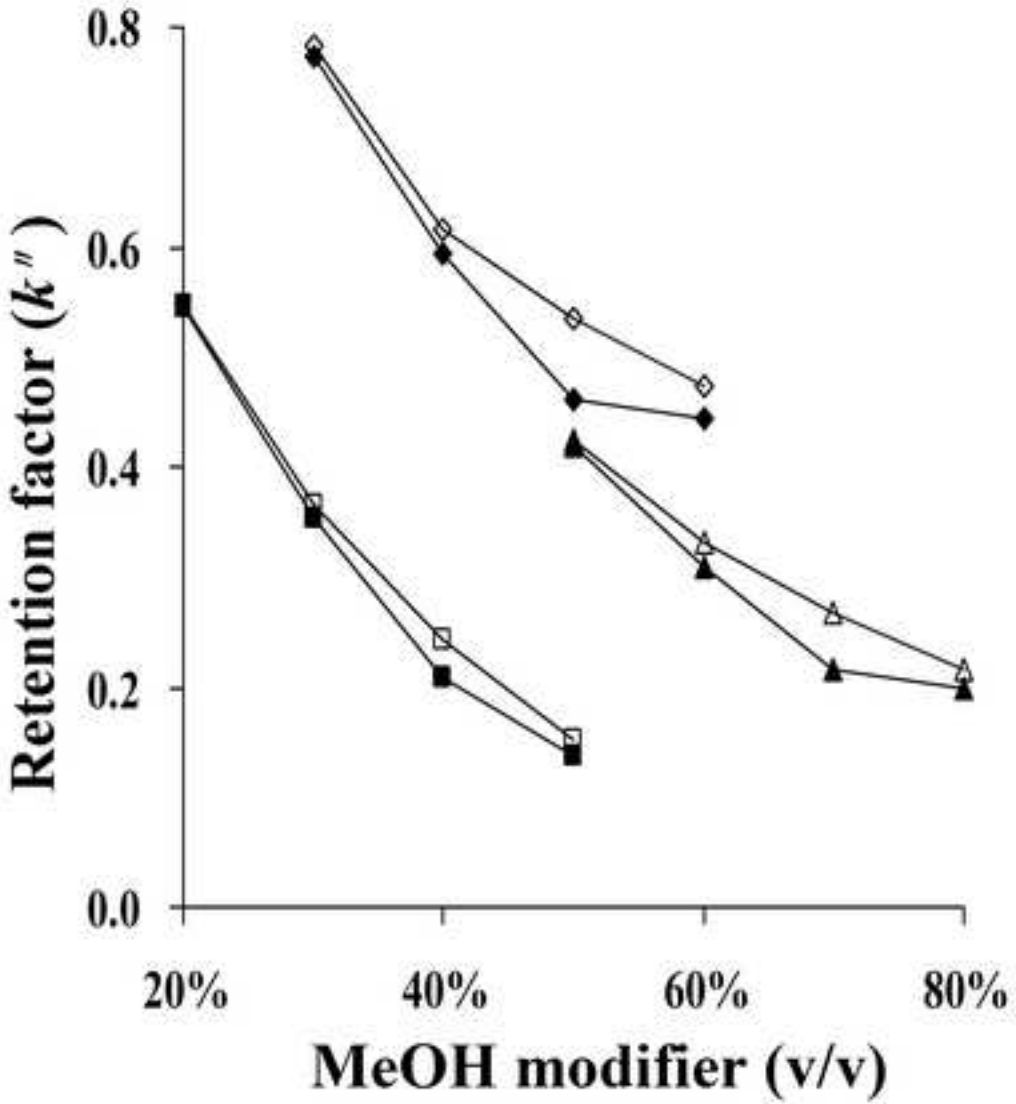

Figure-2

Click here to download high resolution image

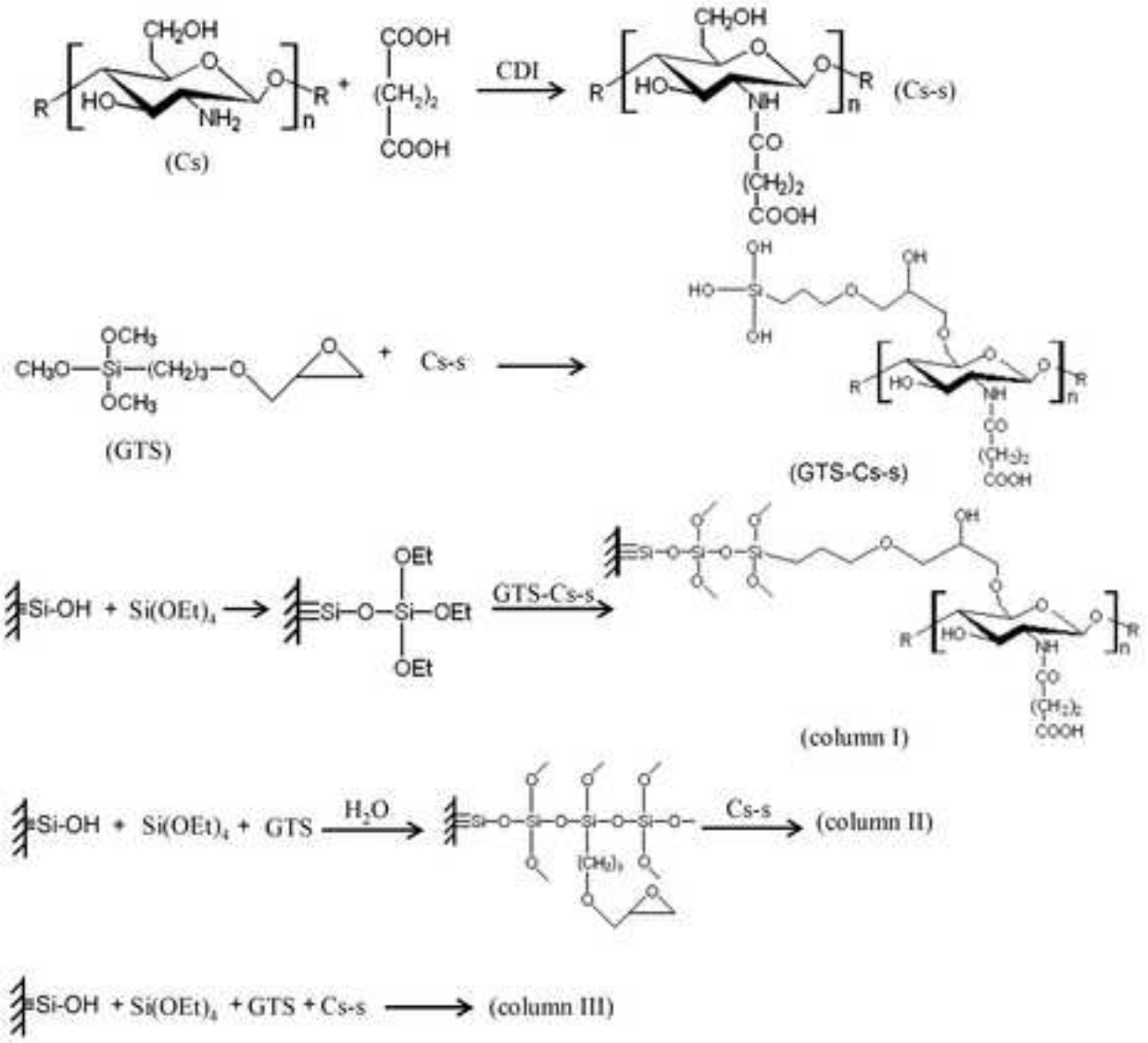

Figure-5

Click here to download high resolution image

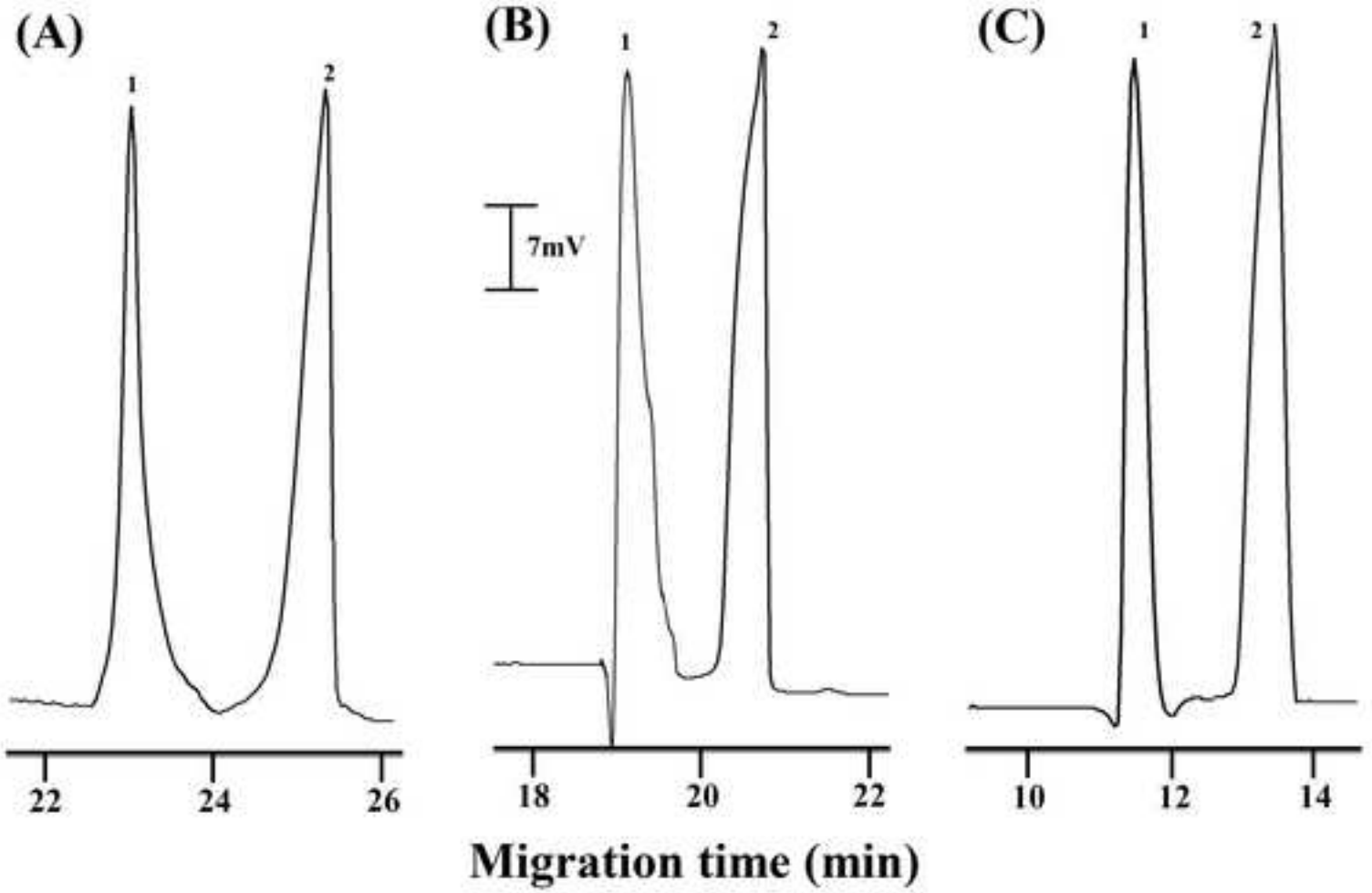

Figure-6

Click here to download high resolution image

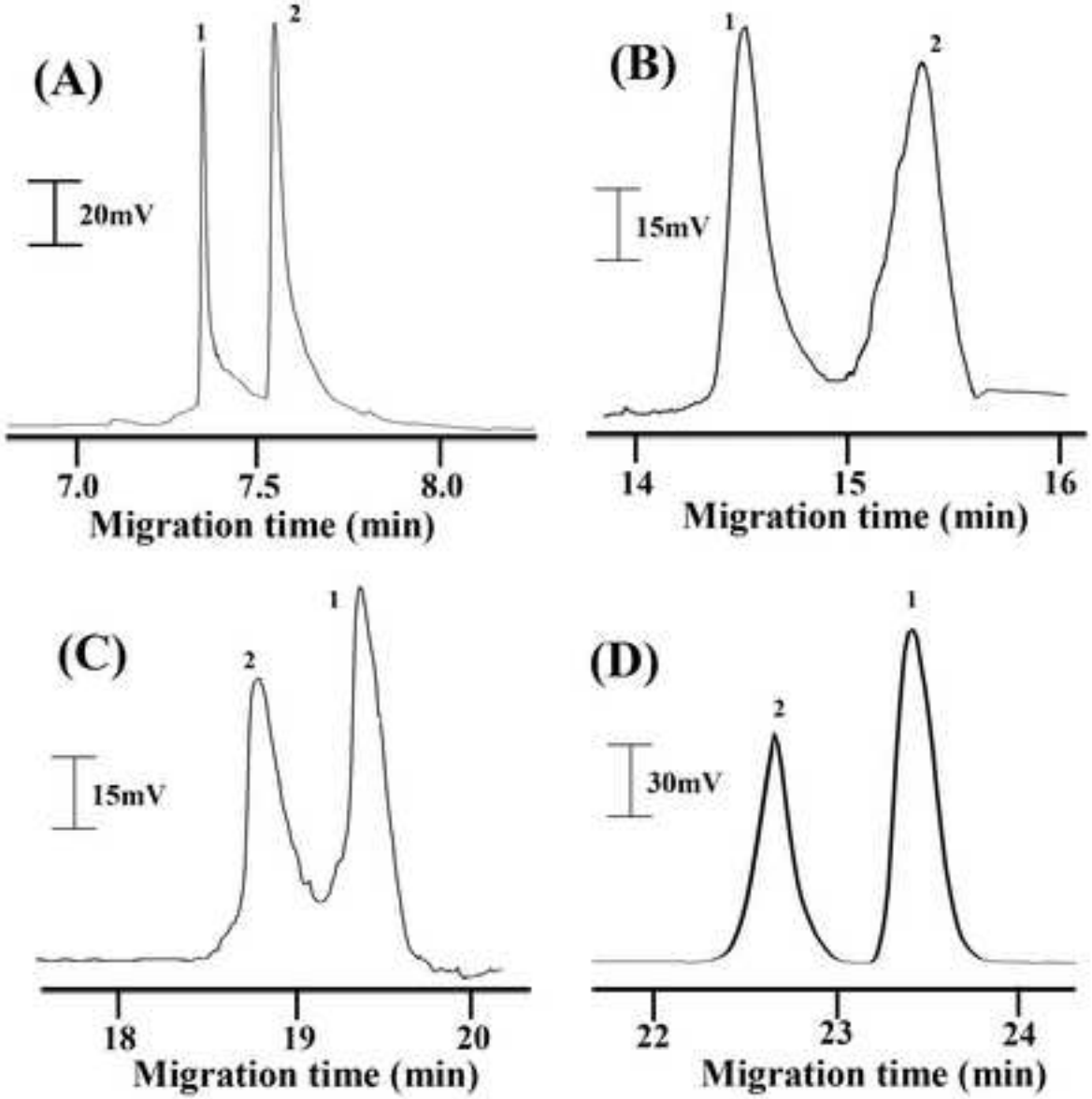

Figure-9

Click here to download high resolution image